Pure appl. geophys. 165 (2008) 1–24
DOI 10.1007/s00024-008-0401-1

Pure and Applied Geophysics

Characteristics of Soil Response in Near-Fault Zones during the 1999 Chi-Chi, Taiwan, Earthquake

O. V. PAVLENKO

Abstract—Distribution of parameters characterizing soil response during the 1999 Chi-Chi, Taiwan, earthquake (M_w = 7.6) around the fault plane is studied. The results of stochastic finite-fault simulations performed in PAVLENKO and WEN (2008) and constructed models of soil behavior at 31 soil sites were used for the estimation of amplification of seismic waves in soil layers, average stresses, strains, and shear moduli reduction in the upper 30 m of soil, as well as nonlinear components of soil response during the Chi-Chi earthquake. Amplification factors were found to increase with increasing distance from the fault (or, with decreasing the level of "input" motion to soil layers), whereas average stresses and strains, shear moduli reduction, and nonlinear components of soil response decrease with distance as $\sim r^{-1}$. The area of strong nonlinearity, where soil behavior is substantially nonlinear (the content of nonlinear components in soil response is more than ~40–50% of the intensity of the response), and spectra of oscillations on the surface take the smoothed form close to $E(f) \sim f^{-n}$, is located within ~20–25 km from the fault plane (~1/4 of its length). Nonlinearity decreases with increasing distance from the fault, and at ~40–50 km from the fault (~ 1/2 of the fault length), soil response becomes virtually linear. Comparing soil behavior in near-fault zones during the 1999 Chi-Chi, the 1995 Kobe (M_w = 6.8), and the 2000 Tottori (Japan) (M_w = 6.7) earthquakes, we found similarity in the behavior of similar soils and predominance of the hard type of soil behavior. Resonant phenomena in upper soil layers were observed at many studied sites; however, during the Chi-Chi earthquake they involved deeper layers (down to ~40–60 m) than during lesser-magnitude Kobe and Tottori earthquakes.

Key words: The 1999 Chi-Chi earthquake, nonlinear soil behavior, seismic wave amplification, stresses, strains, shear moduli reduction, nonlinear components of soil response.

1. Introduction

The Chi-Chi earthquake (M_w = 7.6) that occurred in central Taiwan on September 21, 1999 was recorded by more than 400 strong motion devices island-wide. The majority of near-fault records were obtained at soil sites, and at present they apparently represent the most complete database allowing a study of soil behavior during a strong earthquake in near-fault zones at various distances from the fault.

Institute of Physics of the Earth, Russian Academy of Sciences, B. Gruzinskaya 10, Moscow 123995, Russia. E-mail: olga@ifz.ru

Journal : **24** Dispatch : **17-10-2008** Pages : **24**
Article No. : **0401** ☐ LE ☐ TYPESET
MS Code : **0401** ☑ CP ☑ DISK

In the paper by PAVLENKO and WEN (2008) we simulated acceleration time histories of the Chi-Chi earthquake at rock and soil sites and constructed models of the behavior of upper ~80 m of soil at 31 soil sites located within ~50 km from the fault. At seven sites, such as, TCU065, TCU072, TCU138, CHY026, CHY104, CHY074, and CHY015, information on the profiling data down to ~70–140 m was available. For the other twenty four sites, the profiling data were known down to ~30–40 m, and to construct models of soil behavior, we assumed approximate values of the profiling parameters at depths of ~30–80 m based on shallow *S*-wave velocity structures obtained by LIN *et al*. (2006) for western Taiwan (PAVLENKO and WEN, 2008). To construct models of soil behavior, we used a method similar to that developed for the estimation of soil behavior based on vertical array records (PAVLENKO and IRIKURA, 2003; 2006). As input for soil layers, we used acceleration time histories of the Chi-Chi earthquake, simulated by stochastic finite-fault modeling with a slip distribution over the fault plane obtained by CHI *et al*. (2001). First, we simulated the acceleration time histories of the Chi-Chi earthquake at 18 rock sites, and comparing them with the observed ones, calibrated the calculation program, i.e., found input parameters for the stochastic simulation, such as, parameters of radiation of seismic waves from the source and parameters of their propagation: Geometrical spreading, *Q(f)*, kappa operator describing additional attenuation of the spectra, parameters defining the shape of the time window and some others. The earthquake source (119 km by 35 km) was represented as a set of 85 subfaults of 7 km by 7 km. At the second stage, we simulated acceleration time histories at soil sites, at the bottoms of soil layers. These signals were used as "inputs" to soil layers, i.e., prescribed motion at the base of soil columns (that is, we assumed infinity rigidity in the underlying medium). The technique and the constructed models of soil behavior at 31 soil sites are described in detail in PAVLENKO and WEN (2008). The models represent vertical distributions of hysteretic relations of stresses and strains, induced in the upper tens of meters of soil and changing in time during the strong motion.

Models of soil behavior are constructed for 31 soil sites located at various distances from the fault plane within a wide range of azimuthal directions, and they allow us to obtain a general representation of soil behavior during the Chi-Chi earthquake. With these models, we can investigate some regularities in soil behavior during a strong earthquake at various distances from the fault plane.

In this paper, the constructed models of soil behavior are applied to estimate some parameters, characterizing soil response during the Chi-Chi earthquake, such as, amplification of seismic waves by soil layers, stresses and strains induced by the strong motion in soil layers at different depths, reduction of shear moduli in soil layers due to strong motion, and nonlinear components of soil response. The distribution of these parameters around the fault plane is analyzed.

As shown in the paper by PAVLENKO and WEN (2008), soil behavior during the Chi-Chi earthquake was essentially nonlinear in the near-fault zones, and in this paper, the influence of nonlinearity of soil response on the studied parameters is discussed.

Journal : 24 Dispatch : 17-10-2008 Pages : 24
Article No. : 0401 ☐ LE ☐ TYPESET
MS Code : 0401 ☑ CP ☑ DISK

2. Data and Methods

In this paper, numerical models of soil behavior during the Chi-Chi earthquake at 31 soil sites are used that were constructed and described in PAVLENKO and WEN (2008). Figure 1 shows the locations of the studied soil sites, identifies liquefaction zones, and the area of basin-induced surface waves. Information on the soil sites, such as, the distances to the fault plane and site classification according to LEE *et al*. (2001), as well as estimated parameters of soil response, are given in Table 1. Seven sites, such as, TCU065, TCU072, TCU138, CHY026, CHY104, CHY074, and CHY015, for which

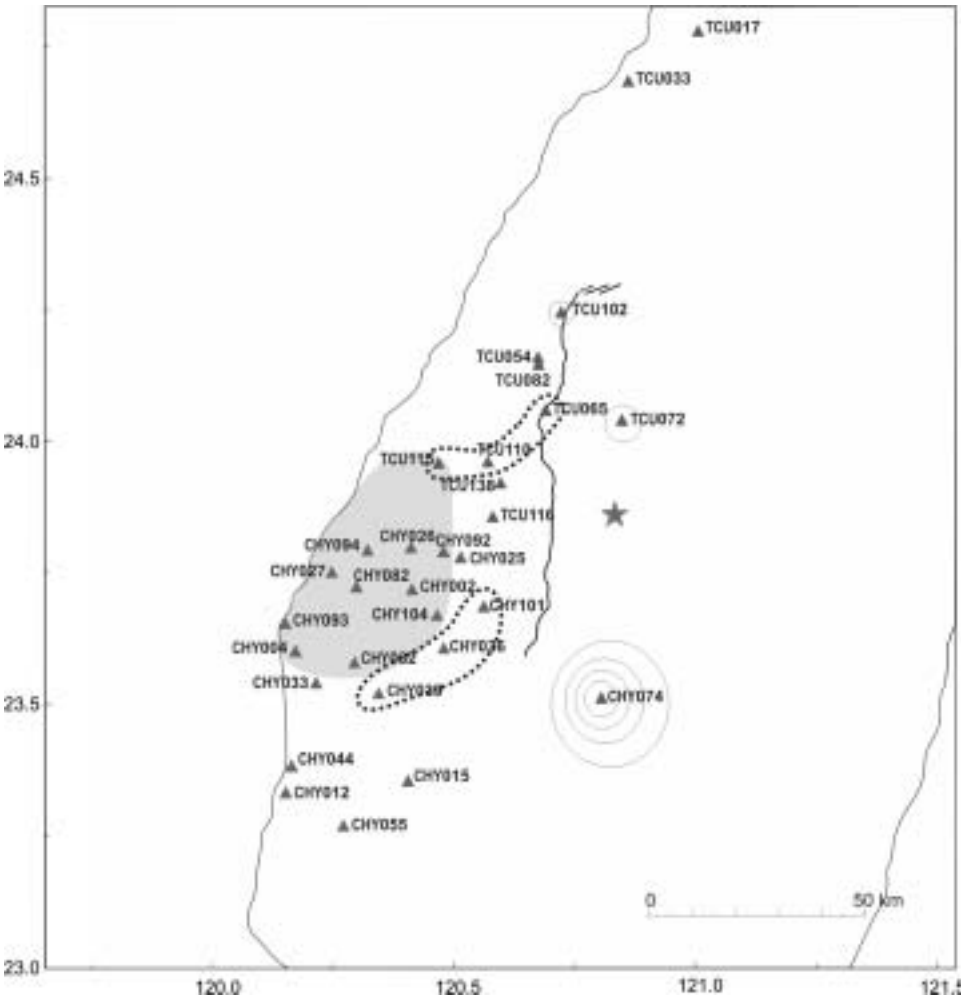

Figure 1
Locations of the studied soil sites around the fault plane of the Chi-Chi earthquake. Dotted lines indicate areas showing signs of soil liquefaction; area of basin-induced surface waves is marked by gray color.

Journal : 24 Dispatch : 17-10-2008 Pages : 24
Article No. : 0401 ☐ LE ☐ TYPESET
MS Code : 0401 ☑ CP ☑ DISK

Table 1

Characteristics of soil response at 31 soil sites during the 1999 Chi-Chi earthquake

Station Code	r, km	$V_{s\text{-}30}$, m/s	F_a	F_v	τ_{30}, Pa	γ_{30}, 10^{-5}	$\Delta G/G_{max\text{-}30}$, %	Nl, %	Site Class (Lee *et al.*, 2001)
CHY101	1.9	260	1.5	2.0	1817	18.0	81	75	D
TCU110	2.4	207	0.7	2.9	1013	32.0	46	57	E
TCU116	3.4	483	1.0	1.8	852	0.3	32	16	E
TCU138	3.8	605	1.1	1.6	2140	0.54	10	24	D
TCU082	5.7	478	1.0	1.7	1162	0.3	15	15	D
CHY025	5.9	277	1.2	2.7	1487	11.5	41	62	E
TCU054	6.1	454	1.1	1.7	1494	0.8	21	11	D
TCU065	6.9	300	2.5	2.9	1677	9.3	63	54	D
CHY036	7.5	282	2.4	2.1	1995	9.6	73	61	D
TCU102	7.8	735	1.4	2.2	2325	3.4	51	56	D
CHY092	9.5	260	1.3	2.5	440	1.2	37	11	E
CHY104	9.5	225	2.2	2.9	1435	5.7	13	28	E
TCU115	11.4	190	1.4	3.1	654	17.0	34	50	E
CHY074	12.8	546	1.6	2.1	1824	3.5	44	25	C
TCU072	14.9	563	2.7	2.1	3481	6.2	37	48	D
CHY002	15.0	231	1.9	2.6	420	0.7	16	28	E
CHY026	16.1	226	1.2	2.0	530	8.0	22	33	E
TCU033	16.9	448	2.3	1.9	1642	0.5	12	22	D
CHY039	20.8	198	2.0	2.2	450	5.8	86	27	E
CHY094	24.9	227	1.6	2.7	1048	4.1	9	16	E
CHY032	25.6	202	3.1	3.2	780	2.9	9	33	E
CHY015	25.9	234	2.2	2.6	361	1.0	19	31	D
CHY082	26.6	209	2.2	3.0	211	0.8	13	25	E
TCU017	29.7	601	2.2	2.3	227	0.2	28	8	?
CHY027	32.1	221	3.9	3.4	645	4.9	13	24	E
CHY033	33.6	194	3.0	3.6	970	5.3	7	13	E
CHY004	38.2	279	2.8	3.0	1342	3.5	7	11	E
CHY093	41.2	199	2.8	3.4	1145	4.7	5	11	E
CHY055	41.5	240	3.7	3.0	1234	3.8	5	12	E
CHY044	43.0	193	3.0	2.9	576	2.2	5	30	E
CHY012	46.6	202	3.5	2.8	276	1.0	2	28	E

more complete information on the profiling data down to $\sim$70–140 m was available, are marked by bold face.

Parameters, characterizing soil response during the Chi-Chi earthquake, were estimated based on the constructed models of soil behavior. Four groups of parameters were studied, such as, (1) characteristics of amplification of seismic waves by soil layers; (2) stresses and strains induced in soil layers by the Chi-Chi earthquake; (3) reduction of shear moduli in soil layers due to strong motion; and (4) contents of nonlinear components in soil response.

Coefficients of amplification of seismic waves by soil layers represent the ratio of the intensity of an observed ground motion to a reference value of that intensity for a particular site condition (intact rock or rock-average). In this paper, amplification factors were estimated separately for acceleration and velocity (from accelerograms and

Journal : 24 Dispatch : 17-10-2008 Pages : 24
Article No. : 0401 ☐ LE ☐ TYPESET
MS Code : 0401 ☑ CP ☑ DISK

velocigrams) as the ratios of root mean-square (*rms*) accelerations and velocities on the surfaces and at the bottoms of soil thicknesses. Values of *rms* accelerations and velocities were calculated for 50-second time intervals of strong motion; estimates obtained for NS and EW components averaged. Amplification was estimated for the same acceleration time histories that were previously used for constructing models of soil behavior (which were taken as one of the series of accelerograms calculated by the stochastic method).

Accelerograms of the Chi-Chi earthquake possess a fairly uniform intensity during the strong motion, and *rms* values should give us rather reliable estimates of the square roots of the ratios of intensities of oscillations on the surfaces and at the bottoms of soil layers. The selected 50-second time intervals correspond to the largest duration of records, observed at southern stations (as mentioned in the paper by PAVLENKO and WEN (2008), directivity effects are clearly seen as decreased durations of acceleration time histories in forward (northern) directions and increased durations in backward (southern) directions; eastern and western directions represent intermediate cases). At stations, located to the north, east and west of the fault plane, the duration of records is smaller, however, these differences (as well as the increase of duration with distance) can only slightly influence amplification estimates, because the ratios are taken of rms values of oscillations on the surfaces and at the bottoms of soil layers. Generation of surface basin waves does not change our estimates of amplification, because the estimates are based on the simulated records on the surfaces and at the bottoms of soil layers and basin waves are not simulated in our one-dimensional problem. In this work, the dependence of amplification on frequency is not studied, because the nonlinearity of soil response was high in near-fault zones and quickly decreased with the distance from the fault. Nonlinear effects change the dependences of amplification coefficients on frequency, and analysis of frequency-dependent amplification would be complicated. We will likely study this problem in the future. Since amplification factors are considered to be functions of the amplitude of shaking, their dependencies on the distance from the fault plane (i.e., on the level of input motion) are studied.

Maximum and average (averaged over the duration of the strong motion) stresses and strains induced by the strong motion in soil layers were estimated. To obtain these estimates, at each site, for each soil layer, maximum (during the strong motion) stresses and strains were found; to find their average estimates, absolute values of "limiting" (for loading and unloading cycles) stresses and strains corresponding to final points of loading and unloading on the hysteretic curves were averaged for each site and for each soil layer; then, averaging was performed over two horizontal components, NS and EW. Average values of stresses and strains were estimated for the upper 30 m of soil most representative from the viewpoint of engineering seismology.

Shear moduli reduction values were assessed for soil layers within the upper 30 m in the following way. For each site, average shear moduli were calculated as the ratios of stresses and strains averaged in time (over the strong motion duration), in depth (over the upper 30 m), and over two horizontal components; stresses and strains were taken as their absolute values corresponding to final points of loading and unloading cycles of the hysteretic curves. Shear moduli reduction was calculated as the difference between

Journal : 24 Dispatch : 17-10-2008 Pages : 24
Article No. : 0401 ☐ LE ☐ TYPESET
MS Code : 0401 ☑ CP ☑ DISK

maximum values of shear moduli, calculated within small time intervals at the beginning parts of the strong motion records, and their average values, normalized by the average values and expressed in percent. As mentioned in PAVLENKO and WEN (2008), due to averaging and smoothing of the models of soil behavior, the obtained shear moduli reduction values could be slightly underestimated. At sites where soil behavior was not adequately simulated in the middle and final parts of the strong motion because of basin effects (Fig. 1), shear moduli reduction estimates should be treated as very approximate.

To estimate the contents of nonlinear components in soil response, methods of nonlinear system identification and the white-noise approach (MARMARELIS and MARMARELIS, 1978) were applied. Application of these methods to seismic data analysis is described in PAVLENKO (2001) and PAVLENKO and IRIKURA (2005). In system analysis, the nonlinear identification of a system implies determination of linear and nonlinear domains of the system response and construction of such a mathematical model of a system that its seismic response coincides with the response of the real physical system. Soil profiles can be represented as nonlinear systems, transforming input seismic signals into the ground response. The quickest and most effective method for nonlinear system identification is testing the studied system with the Gaussian white noise and calculating the Wiener kernels. If an input is the Gaussian white noise, an output can be represented as the Wiener series (MARMARELIS and MARMARELIS, 1978):

$$y(t) = \sum_{m=0}^{\infty} G_m[h_m(\tau_1, \ldots, \tau_m);\, x(t'),\ t' \le t], \tag{1}$$

where G_m are orthogonal functionals, if *x(t)* is the Gaussian white noise with a zero mean, $\{h_m(\tau_1,\ldots,\tau_m)\}$ is a sequence of the Wiener kernels, and $\tau_1,\ldots,\tau_m$ are time delays. The first four Wiener functionals are:

$$G_0[h_0; x(t)] = h_0, \tag{2}$$

$$G_1[h_1; x(t)] = \int_0^{\infty} h_1(\tau) x(t-\tau)\, d\tau, \tag{3}$$

$$G_2[h_2; x(t)] = \int_0^{\infty}\int h_2(\tau_1, \tau_2) x(t-\tau_1) x(t-\tau_2)\, d\tau_1 d\tau_2 - P\int_0^{\infty} h_2(\tau_1, \tau_1)\, d\tau_1, \tag{4}$$

$$\begin{aligned} G_3[h_3; x(t)] = {} & \int_0^{\infty}\int\int h_3(\tau_1, \tau_2, \tau_3) x(t-\tau_1) x(t-\tau_2) x(t-\tau_3)\, d\tau_1 d\tau_2 d\tau_3 \\ & - 3P\int\int_0^{\infty} h_3(\tau_1, \tau_2, \tau_2) x(t-\tau_1) d\tau_1 d\tau_2, \end{aligned} \tag{5}$$

where τ is time delay, P is the intensity of the Gaussian white noise not depending on frequency.

Journal : 24 Dispatch : 17-10-2008 Pages : 24
Article No. : 0401 ☐ LE ☐ TYPESET
MS Code : 0401 ☑ CP ☑ DISK

Terms in the Wiener series are orthogonal with respect to the input signal in the form of the Gaussian white noise, so the Wiener kernels can be determined mutually independent. Effective methods can be used in estimating the Wiener kernels, based on determination of cross-correlation functions, and knowledge of a limited number of these kernels allows the best approximation for a real system from the viewpoint of the minimal mean square error (MARMARELIS and MARMARELIS, 1978). By analogy with an ordinary impulse characteristic $h(t)$, the series of the Wiener kernels $\{h_m\}$ can be treated as a generalized, composed impulse characteristic of a nonlinear system. The first-order kernel defines the linear part of the system response, whereas higher-order kernels describe nonlinear corrections related to quadratic, cubic, and higher-order nonlinearities of the system. The nonlinear corrections express interactions between the values of the input signal in the past with respect to their influence on the response at present. Analyzing the nonlinear components in the output, we can judge regarding the types and quantitative characteristics of the system nonlinearity: If the second Wiener functional G_2 provides the largest contribution to the system response, the system possesses mostly quadratic nonlinearity; if the third functional G_3 contributes more, the system is cubic nonlinear, etc. (MARMARELIS and MARMARELIS, 1978).

Knowledge of stress–strain relations in soil layers in strong ground motion allows calculation of the propagation of testing signals in the studied soil profiles and the nonlinear identification of the soil behavior (PAVLENKO, 2001). Thus, to estimate nonlinear components of soil response, soil profiles were tested by the Gaussian white noise, and estimates of the zero-, first-, second-, and third-order Wiener kernels were constructed based on input and output signals of 500,000 points of duration (more than 40 minutes). Since Wiener kernels and functionals depend on the intensity of an input signal P, the intensity of testing noise signals was chosen so that average stresses and strains induced in soil layers during the propagation of testing signals were close to those induced in the layers by seismic waves from the Chi-Chi earthquake. Based on the estimated Wiener kernels, the response of the linear model and nonlinear corrections accounting for quadratic and cubic nonlinearities of soil response was constructed according to formulas (3)–(5). Zero-order Wiener kernels h_0 describe quasi-static deformations of the surface (related to even-order nonlinearities); they can be interpreted as a result of accumulation of residual shift deformations on the surface (ZVOLINSKII, 1982). They were evaluated as constant parts of soil response; the obtained estimates were averaged over NS and EW components.

Nonlinear components were estimated in percent of the intensity of soil response. The entire nonlinear component of soil response was estimated as the deviation of the real soil response from the response of the linear model constructed by zero- and first-order kernels. The nonlinear quadratic and cubic components were estimated as nonlinear corrections due to quadratic and cubic nonlinearities predicted by kernels $\{h_2\}$ and $\{h_3\}$, respectively. Then the residual part of the soil response was estimated, which is related to higher-order (4th-, 5th-, etc.) nonlinearities, as well as to inaccuracies in estimating kernels (MARMARELIS and MARMARELIS, 1978; PAVLENKO, 2001).

Journal : 24 Dispatch : 17-10-2008 Pages : 24
Article No. : 0401 ☐ LE ☐ TYPESET
MS Code : 0401 ☑ CP ☑ DISK

In this paper, the dependence of the above described parameters of soil response during the Chi-Chi earthquake on the distance from the fault plane is analyzed. All studied soil sites are located in near-fault zones, and their distances from the fault plane are comparable with the fault length. Generally speaking, two values can be considered as the distance of a site from the earthquake source, such as, the shortest distance of a site from the fault plane and the average distance of a site from all subfaults of the fault plane (or weighted average distance with weights being proportional to subfault radiation intensities). It was found that the dependencies of the studied parameters on their distance from the source can be approximated by power functions, and these approximations are more exact (scattering of the obtained estimates is smaller), when we define "distance from the source" as the shortest distance of a site from the fault plane. Therefore, later on distance from the fault r designates the shortest distance of a site from the fault plane.

Inaccuracies in the obtained estimates of soil response parameters are mainly caused by deviations of the constructed models of soil behavior from real soil behavior, by inaccuracies in the profiling data, and by errors in the obtained estimates of the Wiener kernels and functionals.

3. Results

Table 1 summarizes information of the studied soil sites (closest distances to the fault plane, average S-wave velocities in the upper 30 m of soil, $V_{s\text{-}30}$, site classification according to LEE *et al.* (2001) and the obtained estimates of soil response parameters, such as amplification factors for acceleration and velocity, average stresses, strains, and shear moduli reduction in the upper 30 m of soil, as well as the contents of nonlinear components in soil response.

As seen from the Table, the majority of sites (22 sites) possesses soft soils in the upper 30 m: $V_{s\text{-}30}$ is less than 300 m/s, whereas at the other 9 sites possessing denser subsurface soils $V_{s\text{-}30}$ varies within 448–735 m/s. Thus in many cases it was found reasonable to consider separately these two groups of sites, such as sites with "softer" subsurface soils ($V_{s\text{-}30} \leq 300$ m/s) and sites with "harder" subsurface soils ($V_{s\text{-}30} \geq 450$ m/s). Simultaneously, the whole number of the studied sites is not large and virtually all of them are located in valleys to the west of the fault, so that further division of them into smaller groups considering the age and composition of soil layers is not reasonable.

3.1. Amplification of Seismic Waves in Subsurface Soils in Near-Fault Zones during the Chi-Chi Earthquake

The constructed models of soil behavior allowed a rather detailed study of amplification of seismic waves by subsurface soils during strong ground motion. Amplification factors were estimated for acceleration and velocity (F_a and F_v); the results

Journal : 24 Dispatch : 17-10-2008 Pages : 24
Article No. : 0401 ☐ LE ☐ TYPESET
MS Code : 0401 ☑ CP ☑ DISK

are presented in Figure 2 and in Table 1. In Figure 2, in the upper raw, the distributions of root-mean-square accelerations at the "inputs" to soil layers a_{rms} are shown (Fig. 2a), as well as amplification of seismic waves by soil layers for acceleration F_a (Fig. 2b), and $V_{s\text{-}30}$ (Fig. 2c). Below, there are plots showing the obtained estimates of root-mean-square accelerations and velocities a_{rms} and v_{rms} (Fig. 2d) and amplification factors for acceleration and velocity, F_a and F_v (Fig. 2e), as functions of the distance from the fault; their approximations by power and linear functions are also shown. In the lower row, we can see the dependencies of the obtained amplification factors on the level of "input" motion to soil layers (i.e., on a_{rms} and v_{rms}, respectively) (Fig. 2f) and on $V_{s\text{-}30}$ (Fig. 2g), as well as the dependency of rms accelerations on the surfaces $(a_{\text{rms}})^{\text{S}}$ on rms accelerations at the bottoms of soil layers a_{rms} (Fig. 2h). Thus, the obtained results allow us to analyze the influence of various factors on the values of amplification of seismic waves by soil layers.

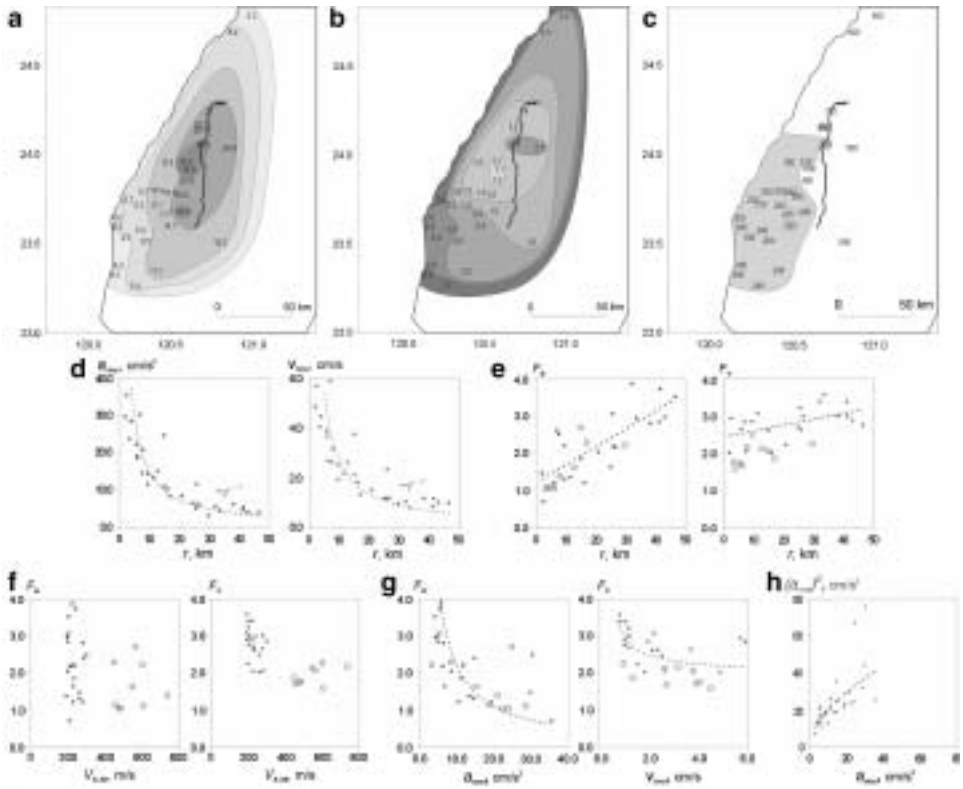

Figure 2

Upper raw: distribution around the fault plane of (a) – "input" motion to soil layers (rms accelerations at the bottoms of soil layers) a_{rms}, (b) – factors of amplification of seismic waves by soil layers for acceleration F_a, (c) – average S-wave velocities in the upper 30 m $V_{S\text{-}30}$. Lower raw: (d) – "input" motion to soil layers a_{rms}, (e) – amplification factors for acceleration and velocity F_a and F_v as functions of the distance from the fault.

Journal : 24 Dispatch : 17-10-2008 Pages : 24
Article No. : 0401 ☐ LE ☐ TYPESET
MS Code : 0401 ☑ CP ☑ DISK

Values of $a_{\rm rms}$ and $v_{\rm rms}$ decrease with increasing distance from the fault plane as $\sim r^{-1}$ (Fig. 2d), which corresponds to theoretical decrease of amplitudes due to geometrical spreading. Amplification factors F_a and F_v are greater than 1 and smaller than 4 for virtually all the sites (Fig. 2b, e-g; Table 1). As seen from the figures, amplification increases with distance (Fig. 2d), i.e., with decreasing amplitudes of "inputs" to soil layers, $a_{\rm rms}$, which is clearer for acceleration than for velocity. Linear functions can be used as approximating ones, however, scattering of the obtained estimates around linear regression lines is rather large, and it can be due to different factors.

As known, three main mechanisms of seismic wave transformation in subsurface soils are: (1) Transition of seismic waves to upper soil layers with (usually) smaller values of $V_{s\text{-}30}$ and density, ρ, leading to amplification of seismic oscillations according to energy conservation law, (2) resonant phenomena the upper softer soil layers also leading to amplification, (3) nonlinearity of soil response, often leading to de-amplification of seismic oscillations.

To evaluate the influence of different mechanisms on amplification of seismic waves in soil layers during the Chi-Chi earthquake, let us consider separately sites with "softer" and "harder" subsurface soils (in Figs. 2e–g they are shown by points and circles, respectively). As seen from the figure, amplification factors for acceleration, F_a, at "softer" and "harder" soil sites are close to each other, and can be approximated by the same function of the distance from the fault (or of the level of "input" motion), whereas, amplification factors for velocity, F_v, are substantially smaller at "harder" subsurface soils than at "softer" soils. This is clearly seen from Figure 2f and agrees with seismological observations that "peak ground velocity and displacement show higher amplifications for soil sites than for rock sites (in our case, softer soil sites and harder soil sites), while peak ground acceleration is roughly independent of the site classification" (AKI and IRIKURA, 1991) (that is, does not show higher amplification at soft soil sites).

The obtained results are in a good agreement with the dependencies of amplification factors on the intensity of ground motion and on average S-wave velocities in upper 30 m of soil described in the paper by STEWART *et al.* (2001). The authors discuss general regularities of reduction of amplification factors with increasing $V_{s\text{-}30}$ or reference motion amplitude, obtained by various researchers for various strong earthquakes. Preliminary data on the 1999 Chi-Chi earthquake, obtained by STEWART *et al.*, are also in agreement with the results of this work (Fig. 2g).

The observed dependencies of amplification factors on the level of "input" motion to soil layers is evidently due to the influence of nonlinearity of soil response, which is higher closest to the fault sites. At rather long distances from the fault ($\sim$40–50 km), amplification factors F_a and F_v are close to each other (Fig. 2e), whereas at short distances, nonlinearity of soil response substantially decreases amplification for acceleration and, to a lesser extent, for velocity. This can be due to nonlinear transformations of seismic waves propagating in soil layers: Their spectra tend to take the form $E(f) \sim f^{-n}$, when the high- and medium-frequency spectral components are decreased and the low-frequency

Journal : 24 Dispatch : 17-10-2008 Pages : 24
Article No. : 0401 ☐ LE ☐ TYPESET
MS Code : 0401 ☑ CP ☑ DISK

components remain virtually at the same level. Obviously, the effect is stronger for accelerations than for velocities and displacements.

In the paper by PAVLENKO and WEN (2008), it was concluded that at the majority of soil sites, soil behavior during the Chi-Chi earthquake was defined by resonant oscillations induced in soil layers (in the upper 40–60 m) during strong motion and by nonlinearity of soil response.

At near-fault sites, subsurface water-saturated sandy soils possess hard-type nonlinearity, where de-amplification of seismic oscillations due to nonlinear damping can be rather small, because: (1) Stresses in soil layers rapidly increase at large strains (especially, in near-fault zones) due to pore-pressure build-up (and therefore, accelerations also increase); (2) nonlinear damping (which is proportional to areas within hysteretic curves) can be rather small, as at TCU065 site, for example (PAVLENKO and WEN, 2008). As a consequence, in near-fault zones in sandy water-saturated soils possessing hard-type nonlinearity, de-amplification of seismic oscillations due to nonlinearity often cannot compensate their amplification stipulated by the other two (linear) mechanisms; as a whole, we observe amplification of oscillations on the surface. This is clearly seen, for example, in vertical array records of the 1995 Kobe earthquake at SGK site: in the upper $\sim$11 m of sandy soils possessing hard-type nonlinearity seismic oscillations were noticeably amplified, peak accelerations increased from 0.2–0.3 g at depths of $\sim$25 m and 100 m up to $\sim$0.7 g on the surface. At the same time at the Port Island site, liquefied surface soils possessing soft-type nonlinearity substantially de-amplified seismic oscillations, especially their high-frequency components; peak accelerations at 83 m, 32 m, 16 m, and on the surface were almost similar, $\sim$0.4–0.5 g (PAVLENKO and IRIKURA, 2003).

Thus, amplification factors can be rather large even in cases of strong nonlinearity (at high levels of "input" motion, in near-fault zones) at sites possessing hard-type nonlinearity of subsurface soils, which is clearly seen in Figure 2b: at TCU065 and TCU072 sites located very close to the fault plane, amplification factors are rather high, $F_a \sim$ 2.5–2.7.

Figure 2h shows the obtained estimates of rms accelerations on the surfaces of soil, $(a_{\mathrm{rms}})^S$, versus estimates of rms accelerations at the bottoms of soil layers, a_{rms}. This figure can be compared to the well-known findings of Idriss (1990), such as, plots peak ground acceleration (PHA) on rock versus PHA on soft soil (accounting for the fact that peak accelerations correlate well with rms accelerations, at least, in the case of the Chi-Chi earthquake). As a whole, the dependence shown in Figure 2h agrees well with Idriss's data, but two points with increased $(a_{\mathrm{rms}})^S$ values attract attention, which correspond to TCU065 and TCU072 sites, where subsurface soils possess strong hard-type nonlinear behavior. Our previous experience in studying soil behavior during strong earthquakes shows that we can mostly find areas in the closest vicinities of the fault plane, where soils possess such behavior.

Amplification of oscillations on the surface resulting from resonant phenomena in subsurface soils and hard-type soil nonlinearity are also observed at other near-fault sites,

Journal : 24 Dispatch : 17-10-2008 Pages : 24
Article No. : 0401 ☐ LE ☐ TYPESET
MS Code : 0401 ☑ CP ☑ DISK

such as, CHY101 ($F_a \sim 1.5$), CHY036 ($F_a \sim 2.4$), TCU102 ($F_a \sim 1.4$), CHY104 ($F_a \sim 2.2$), TCU115 ($F_a \sim 1.4$), CHY074 ($F_a \sim 1.6$), CHY002 ($F_a \sim 1.9$), etc.

"Hard" character of soil response nonlinearity virtually disappears at distances of more than $\sim$12–15 km from the fault plane (PAVLENKO and WEN, 2008), because of the decrease of "input" motion intensity. At rather long distances from the fault, amplification of seismic oscillations results from the two above described linear mechanisms; whereas nonlinear effects decrease with distance and can no longer effectively de-amplify seismic oscillations.

3.2. Stresses and Strains Induced in Soil Layers in Near-Fault Zones During the Chi-Chi Earthquake

Analyzing stresses and strains induced in soil layers by the Chi-Chi earthquake, it is also reasonable to distinguish sites with "softer" ($V_{s\text{-}30} \leq 300$ m/s) and "harder" ($V_{s\text{-}30} \geq 450$ m/s) subsurface soils. Figure 3 represents estimated average (upper rows) and maximum (lower rows) stresses and strains induced in soil layers at the studied sites during the Chi-Chi earthquake. Names of sites possessing "harder" subsurface soils are underlined. We can see from the figures that closest to the fault plane sites (within $\sim$20 km from the fault), resonant phenomena are observed in the upper soft soil layers (down to $\sim$40–60 m), i.e., trapping of seismic waves due to the impedance contrast between softer and neighboring denser layers. Stresses in soil layers increased with depth, whereas maximum strains usually occurred in the upper 15–40 m of soil (Fig. 3).

At sites where soft surface layers with $V_{s\text{-}30} \leq 300$ m/s were underlayed by denser layers, and impedance contrast was higher, resonant phenomena were more pronounced. Maximum strains were achieved closest to the fault plane sites, such as, TCU065, TCU110, TCU115, CHY101 ($\sim$0.6–0.8%), CHY025, and CHY036 ($\sim$0.4–0.6%). At other sites maximum strains in soil layers did not exceed $\sim$0.1–0.4%. In the paper by PAVLENKO and WEN (2008), it is concluded that liquefaction phenomena occurred at TCU065, TCU110, TCU115, CHY101, CHY036, and CHY039 sites.

The obtained estimates of average stresses and strains induced in the upper 30 m of soil during the strong motion, τ_{30} and γ_{30}, are given in Table 1, and the distributions of these parameters around the fault plane are shown in Figure 4a and 4b. As seen from the figures, areas of softer subsurface soils with $V_{s\text{-}30} \leq 300$ m/s in Bajada, to the west of the fault, correspond to zones of decreased stresses and increased strains.

Average stresses and strains in the upper 30 m of soil, τ_{30} and γ_{30}, are shown as functions of the distance from the fault (Fig. 4d) and as functions of the level of "input" motion to soil layers, rms accelerations a_{rms} (Fig. 4f). At sites with "softer" subsurface soils (shown by points in the figures), average stresses and strains decrease with distance (in Fig. 4d, the corresponding approximations by functions $\sim r^{-1}$ are shown), and they increase with the level of "input" motion, however scattering of estimates around approximating linear functions is rather large. At sites possessing "harder" subsurface soils, average stresses and strains (shown by circles) deviate from power functions and

Journal : 24 Dispatch : 17-10-2008 Pages : 24
Article No. : 0401 ☐ LE ☐ TYPESET
MS Code : 0401 ☑ CP ☑ DISK

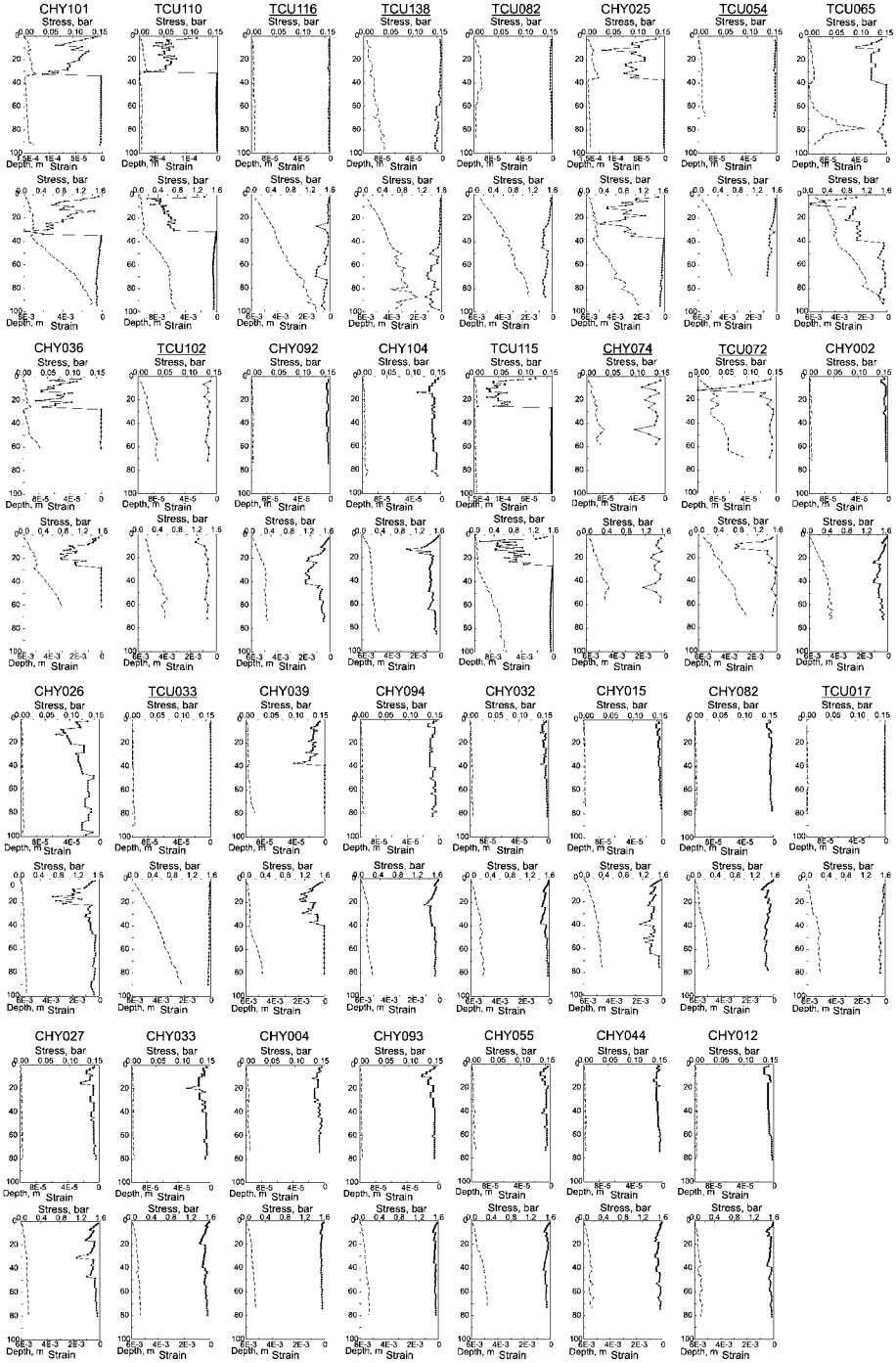

Journal : 24 Dispatch : 17-10-2008 Pages : 24
Article No. : 0401 ☐ LE ☐ TYPESET
MS Code : 0401 ☑ CP ☑ DISK

◄ Figure 3
Estimated average (upper rows) and maximum (lower rows) stresses (dash lines) and strains (solid lines), induced in soil layers during the Chi-Chi earthquake. Stations possessing "harder" subsurface soils are underlined.

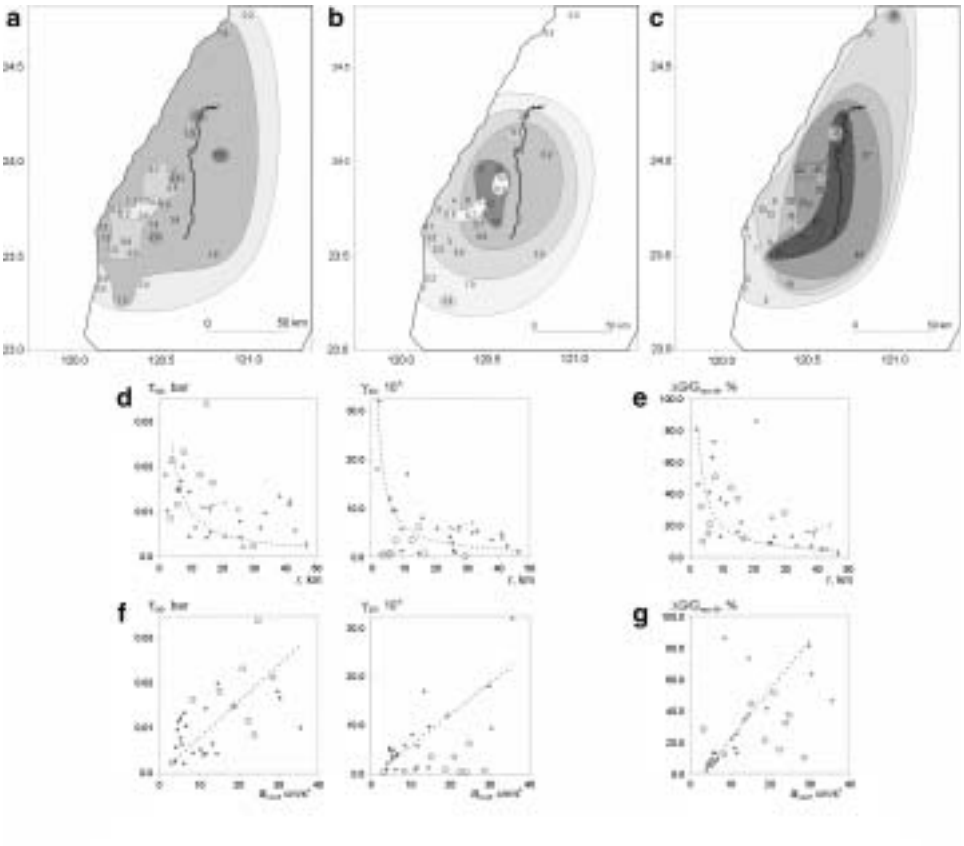

Figure 4
Upper raw: distribution around the fault plane of (a) – average stresses in the upper 30 m of soil τ_{30}, (b) – average strains in the upper 30 m of soil γ_{30}, (c) – estimates of shear moduli reduction in the upper 30 m of soil $\Delta G/G_{max\text{-}30}$ (dotted lines indicate areas showing signs of soil liquefaction). Lower raw: (d) – average stresses τ_{30}, (e) – average strains γ_{30}, (f) – estimates of shear moduli reduction $\Delta G/G_{max\text{-}30}$ as functions of the distance from the fault.

appreciably increase scattering. At these sites, average stresses are higher and average strains are lower than at sites with "softer" subsurface soils.

Evidently, average stresses and strains in the upper soil layers depend on the distance from the fault plane (or the level of "input" motion), as well as on the mechanical parameters of a soil (initially, S-wave velocities and densities). Stresses and strains naturally decrease with increasing distance from the fault, and, at the same time,

Journal : 24 Dispatch : 17-10-2008 Pages : 24
Article No. : 0401 ☐ LE ☐ TYPESET
MS Code : 0401 ☑ CP ☑ DISK

stresses τ_{30} increase, and strains γ_{30} decrease with increasing $V_{s\text{-}30}$. Decreased stress values at some sites in the vicinity of the fault (for example, at CHY092 and CHY002) are obviously related to decreased $V_{s\text{-}30}$ values in the upper layers at these sites, whereas decreased strain values at some other sites (for example, at TCU116, TUC138, TCU082, and TCU054) are due to relatively high $V_{s\text{-}30}$ in the upper soil layers at these sites.

Thus, according to the obtained estimates, at sites possessing "softer" soils, average strains decrease with distance from the fault more quickly than average stresses, probably because stresses in soil layers are defined to a larger extent by radiation from the earthquake source (level of "input" motion to soil layers) than by mechanical properties of soils, whereas strains depend more on soil properties, i.e., on resonant phenomena in upper soil layers.

3.3. Shear Moduli Reduction in Soil Layers in Near-Fault Zones during the Chi-Chi Earthquake

As concluded in PAVLENKO and WEN (2008), closest to the fault plane sites soil behavior during the Chi-Chi earthquake was substantially nonlinear. Nonlinearity of soil response can be characterized by reduction of shear moduli in soil layers (PAVLENKO and IRIKURA, 2005). Thus, the constructed models of soil behavior were used to estimate shear moduli reduction in the upper 30 m of soil, $\Delta G/G_{\max\text{-}30}$. The obtained estimates are presented in Table 1; Figure 4c, e, g show the distribution of $\Delta G/G_{\max\text{-}30}$ estimates around the fault plane, and the dependencies of the estimates on the distance from the fault and on the level of "input" motion to soil layers, respectively.

The evaluated values of $\Delta G/G_{\max\text{-}30}$ testify to high nonlinearity of soil response during the Chi-Chi earthquake: In the closest vicinity of the fault plane, at TCU110, CHY025, TCU065, TCU102, and CHY074 sites, shear moduli reduction in the upper 30 m achieved $\sim$40–50% (Figs. 4c, e; Table 1). The highest $\Delta G/G_{\max\text{-}30}$ values were obtained at CHY101, CHY036, and CHY039 sites, where the constructed models of soil behavior show substantial differences in the shapes of stress-strain curves at the beginning and end of the strong motion, indicating softening (probably, liquefaction) of surface layers. This area is marked by a dotted line in Figures 1 and 4c.

High values of shear moduli reduction $\Delta G/G_{\max\text{-}30} \sim$30–50% were obtained in the closest vicinity of the fault (within $\sim$25 km from the surface rupture) at "soft" soil sites: TCU102, TCU110, TCU115, TCU072, CHY074, TCU116, CHY025, and CHY092 (Fig. 4c). At sites TCU138, TCU082, TCU054, and TCU033, possessing "harder" subsurface soils ($V_{s\text{-}30} \sim$ 450–605 m/s), lower values of shear moduli reduction were obtained: $\Delta G/G_{\max\text{-}30} \sim$ 10–20%. At sites CHY104, CHY002, CHY026, CHY094, and CHY032, shear moduli reduction can be underestimated because of the presence of basin-induced surface waves in records (Fig. 1), which noticeably increases amplitudes of oscillations on the surface and cannot be simulated in our one-dimensional problem (PAVLENKO and WEN, 2008).

Journal : 24 Dispatch : 17-10-2008 Pages : 24
Article No. : 0401 ☐ LE ☐ TYPESET
MS Code : 0401 ☑ CP ☑ DISK

With increasing distance from the fault, shear moduli reduction values decrease to $\sim 10\%$ at 35–50 km and to $\sim 5\%$ at 50–70 km from the fault (Figs. 4c, e), where soil response becomes virtually linear.

In Figures 4e, g shear moduli reduction values for "softer" and "harder" sites are shown by points and by circles, respectively. It is seen from the plots that shear moduli reduction estimates at "softer" sites decrease with distance approximately as $\sim r^{-1}$ and they grow in proportion to the level of "input" motion to soil layers. Points, noticeably deviating from the approximating functions, correspond to CHY039 and CHY036 sites with increased $\Delta G/G_{\max\text{-}30}$, where the constructed models of soil behavior show liquefaction phenomena, and to CHY074 site with decreased $\Delta G/G_{\max\text{-}30}$, possessing dense soils (Class C). As seen from the plots, $\Delta G/G_{\max\text{-}30}$ estimates at "harder" sites substantially increase scattering of points around the approximating relationships (Figs. 4e,g).

Thus, reduction of shear moduli in the upper 30 m of soil at "softer" sites can be rather accurately described as a function inversely proportional to the distance from the fault, $\sim r^{-1}$ and as a linear function of the level of "input" motion, a_{rms}. As mentioned above, strong ground motion during the Chi-Chi earthquake induced resonant amplification of seismic oscillations in the upper soft layers at many sites, and since soil conditions were similar at soil sites located mostly to the south and south-west of the fault (Fig. 1), average strains in the upper 30 m are proportional to the level of "input" motion to soil layers, and their decrease with distance from the fault can be approximately described as $\sim r^{-1}$. Accordingly, shear moduli reduction values depend on distance and on the level of "input" motion in the same manner.

At the same time, at sites with "harder" subsurface soils, resonant phenomena were not observed in the upper 30 m of soil (according to our estimates, maximum strains at these sites correspond to depths of ~ 40 m and more (Fig. 3)), and estimates of shear moduli reduction depend not only on the distance from the fault (or on the level of "input" motion), but, to a greater extent than for "softer" soils, on the profiling data, which are very diverse at these sites, dispersed over a large area around the fault. Consequently, shear moduli reduction values can be quite different, even at sites located equidistant from the fault.

3.4. Nonlinear Components of Soil Response in Near-Fault Zones during the Chi-Chi Earthquake

To estimate nonlinear components of soil response, models of soil behavior constructed in PAVLENKO and WEN (2008) were tested by the Gaussian white noise. Linear and nonlinear components of soil response were distinguished, and their intensities were estimated in percent of the entire intensity of the response.

The obtained estimates are presented in Table 1, and in Figure 5. Figures 5a–c represent the distributions of the estimates of the whole nonlinear component, *Nl*, nonlinear quadratic, *nl-2*, and cubic, *nl-3*, components of soil response, respectively, in the

Journal : 24 Dispatch : 17-10-2008 Pages : 24
Article No. : 0401 ☐ LE ☐ TYPESET
MS Code : 0401 ☑ CP ☑ DISK

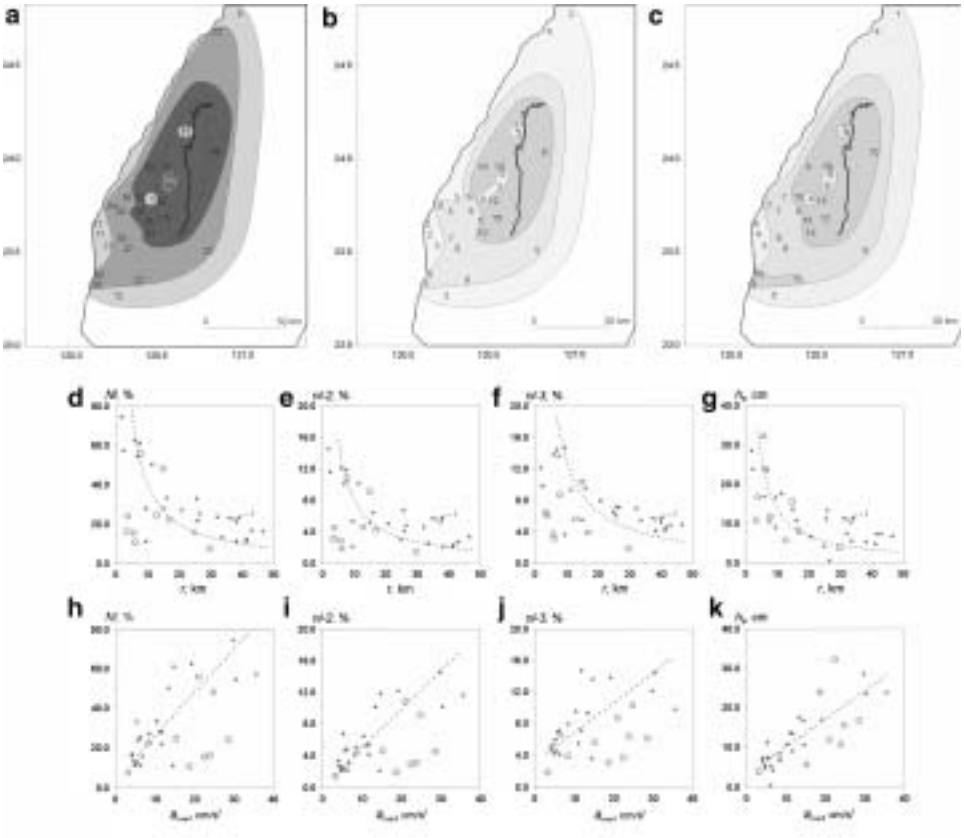

Figure 5
Upper raw: distribution around the fault plane of (a) – whole nonlinear components of soil response *Nl*, (b) – nonlinear quadratic components *nl-2*, (c) – nonlinear cubic components *nl-3*. Lower raw: (d) – whole nonlinear components of soil response *Nl*, (e) – nonlinear quadratic components *nl-2*, (f) – nonlinear cubic components *nl-3*, (g) – quasi-static deformations of the surface h_0 as functions of the distance from the fault.

vicinity of the fault plane. Below in Figures 5d–k, estimates of *Nl*, *nl-2*, and *nl-3*, and the constant component of soil response, h_0, are shown as functions of the distance from the fault r and of the level of "input" motion to soil layers a_{rms}. Values obtained for sites with "softer" and "harder" subsurface soils are shown by points and circles, respectively.

Soft soils in the closest vicinity of the fault possess the highest nonlinearity of the response: According to our estimates, the whole nonlinear components of soil response achieve $Nl \sim 60$–80%, and nonlinear quadratic and cubic components are up to ~ 12–16% of the intensity of the response. At the same time, nonlinear residual components of soil response related to higher-order nonlinearities (the 4th order and higher) are also high, up to ~ 30–40% of the intensity of the response. Evidently, this indicates very high nonlinearity of soil response in near-fault zones during the Chi-Chi earthquake.

Journal : 24 Dispatch : 17-10-2008 Pages : 24
Article No. : 0401 ☐ LE ☐ TYPESET
MS Code : 0401 ☑ CP ☑ DISK

Note that nonlinear quadratic and nonlinear cubic components (their ratio indicates the ratio of even-order and odd-order nonlinear components in soil response) are almost equal closest to the fault (i.e., in conditions of high nonlinearity), however, with increasing distance from the fault (that is, decreasing nonlinearity), nonlinear cubic components become predominant (Figs. 5e, f).

With increasing distance from the fault plane, nonlinear components of soil response decrease, and their dependence on distance can be described in the same manner as for other parameters, such as, approximately $\sim r^{-1}$. Accounting for sites possessing "harder" subsurface soils substantially increases scattering of points around the approximating functions. For sites with "softer" subsurface soils, the dependencies of the obtained estimates of nonlinear components on the level of "input" motion can be approximately described by linear functions (Figs. 5h–k). This is in agreement with our representations of soil nonlinearity: at soft soils, manifestations of nonlinearity increase with the level of "input" motion, i.e., with approach to the fault.

At two closest to the fault plane sites possessing "harder" subsurface soils, such as, TCU072 and TCU102, nonlinearity of soil response was also high, evidently because of expressed resonant phenomena in the upper soft soil layers. At TCU072 site, resonant amplification of seismic oscillations occurred in the upper $\sim$11 m of colluvium ($V_S \approx$ 250 m/s), and at TCU102 site, resonant phenomena were related to the upper $\sim$4–6 m of soft silty soils, which were softened during the strong motion. The behavior of these upper soft layers was substantially nonlinear and described by very sloping stress-strain relations (PAVLENKO and WEN, 2008). Since surface soft layers were underlayed by hard breccia (at TCU072) and gravel (at TCU102), average *S*-wave velocities in the upper 30 m were higher than $\sim$300 m/s at both sites, and the sites were assigned as possessing "harder" subsurface soils, however, nonlinear components at these sites satisfy regularities obtained for sites possessing "softer" subsurface soils (Figs. 5d–k).

Quasi-static shift deformations on the surface, h_0, related to nonlinearity of soil response, achieve 20–35 cm closest to the fault plane sites, according to our estimates (Fig. 5g). They decrease approximately as $\sim r^{-1}$ with increasing distance from the fault; in this case, estimates for "softer" and "harder" soil sites possess similar regularity.

With increasing distance from the fault, nonlinearity of soil response decreases and at distances of $\sim$40–50 km ($\sim$1/2 of the length of the fault plane), nonlinear components in soil response do not exceed 10–15%, according to our estimates (Fig. 5d).

A good illustration of changes in the ratios of linear and nonlinear components in soil response with increasing distance from the fault is provided by impulse characteristics of soil layers. They are shown in Figure. 6 and arranged according to their distance from the fault. They are calculated based on acceleration time histories on the surfaces and at the bottoms of soil layers simulated in PAVLENKO and WEN (2008). Impulse characteristics represent estimates of the first-order Wiener kernels, that is, they describe linear parts of soil response. At sites located at lengthy distances

Journal : 24 Dispatch : 17-10-2008 Pages : 24
Article No. : 0401 ☐ LE ☐ TYPESET
MS Code : 0401 ☑ CP ☑ DISK

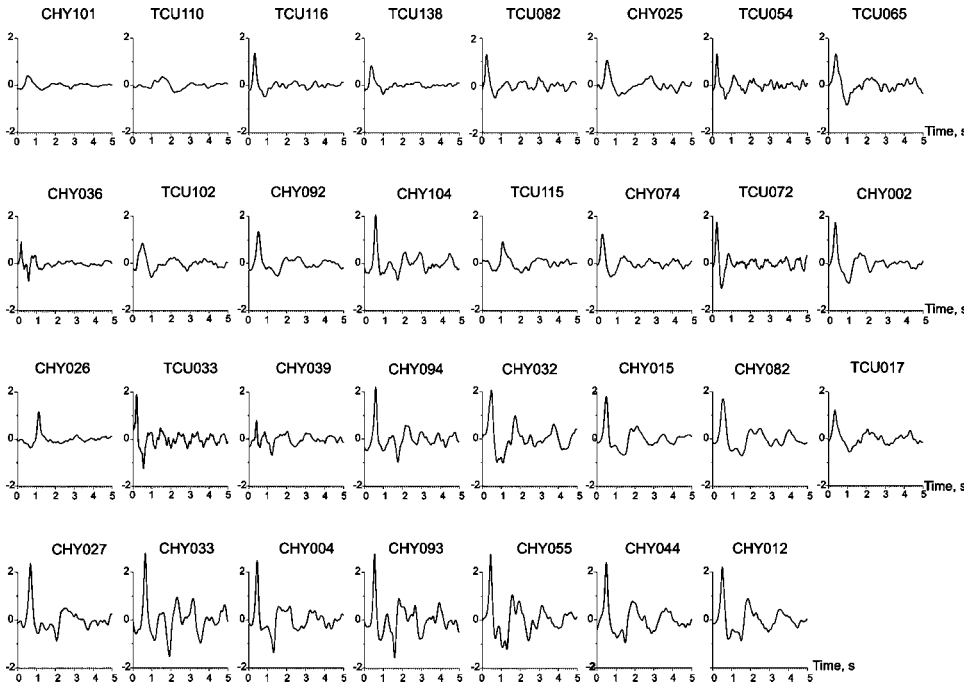

Figure 6
Impulse characteristics of soil response during the Chi-Chi earthquake at the studied soil sites.

from the fault plane, they possess oscillating character, indicating an essential role of resonant phenomena in soil response. With approach to the fault, nonlinear damping increases and the oscillations decrease; impulse characteristics become smoothed and low-frequency, which indicates substantial changes in spectral contents of seismic waves propagating in soil layers, noticeable decrease of linear components and increase of nonlinear components in soil response.

Nonlinearity of soil response during the Chi-Chi earthquake has been studied by ROUMELIOTI and BERESNEV (2003) and by K.-L. Wen (pers. communic.). They investigated spectra of acceleration time histories at soil sites and interpreted lower amplification of seismic waves in some frequency bands during strong ground motions compared to weaker ones (aftershocks) as an indicator of nonlinearity of soil response. ROUMELIOTI and BERESNEV (2003) simulated soil site records using the linear-response assumption whereby the simulated soil site input motions are amplified by weak-motion amplification functions, estimated by the spectral ratio technique from the aftershock records. Their comparison with the observations revealed an average reduction in strong-motion amplification to about 0.5–0.6 of that in weak motions, with an acceleration "threshold" for detectable nonlinearity near 200–300 cm/s^2. However, the authors emphasize a large interstation response variability, which did not allow them to derive a statistically

Journal : 24 Dispatch : 17-10-2008 Pages : 24
Article No. : 0401 ☐ LE ☐ TYPESET
MS Code : 0401 ☑ CP ☑ DISK

significant difference in weak and strong-motion amplifications, based on the responses available at the studied sixteen stations.

4. Discussion and Conclusions

To date, the behavior of subsurface soils down to ~ 100 m during a strong earthquake was thoroughly studied, based on vertical array records of the 1995 Kobe earthquake ($M_w = 6.8$) at three sites (PAVLENKO and IRIKURA, 2002, 2003, 2005) and of the 2000 Tottori earthquake ($M_w = 6.7$) at five sites (PAVLENKO and IRIKURA, 2006).

Only a limited number of vertical array records of strong ground motion are available worldwide, though the database is growing quickly: For example, records of Digital Strong-Motion Seismograph Network Kik-Net (Japan) have been collected since October, 1997 and are accessible through the internet. The majority of strong motion records are made only on the surface, such as in the case of the Chi-Chi earthquake. For the Chi-Chi earthquake, we could simulate rather accurately acceleration time histories at the bottoms of soil layers, at depths of $\sim$70–80 m, and study soil behavior at many sites using methods developed for vertical array records. Thus, the 1999 Chi-Chi earthquake became the third strong earthquake for which models of soil behavior in near-fault zones down to $\sim$70–80 m were constructed PAVLENKO and WEN (2008). At the same time, it is the first strong earthquake for which soil behavior was extensively studied in detail at many sites over a large area within ~ 100 km around the fault plane.

The results presented in this paper, such as estimates of amplification of seismic waves in soil layers, average stresses and strains induced in soil layers by the strong motion, shear moduli reduction and characteristics of nonlinearity of soil response describe soil behavior in near-fault zones during the Chi-Chi earthquake. In spite of the approximate character of the obtained estimates, they allow us to draw conclusions.

As shown above, factors of amplification of seismic waves in subsurface soils estimated for accelerations and velocities increase approximately in proportion to the distance from the fault, $\sim r$. Other estimated parameters decrease with distance (or with a decrease in the level of "input" motion to soil layers). Since the obtained estimates possess a rather large scattering, their behavior was approximated by simple functions. The dependencies of soil response parameters on the level of "input" motion were approximated by linear functions, and their decrease by increasing the distance from the fault – by functions inversely proportional to distance, $\sim r^{-1}$.

Note a slower (than other parameters) decrease of average stresses in soil layers (the upper 30 m) with distance and a large scattering around the approximating curves of the obtained estimates of amplification factors, average stresses and strains, and nonlinear components in soil response (whereas, scattering of $\Delta G/G_{\max\text{-}30}$ estimates is smaller).

Journal : 24 Dispatch : 17-10-2008 Pages : 24
Article No. : 0401 ☐ LE ☐ TYPESET
MS Code : 0401 ☑ CP ☑ DISK

As concluded in PAVLENKO and WEN (2008), the main site effects in near-fault zones of the Chi-Chi earthquake were resonant phenomena in subsurface soils and nonlinearity of soil response. Resonant patterns involved rather thick soil layers, down to ~40–60 m, and noticeably increased strains in upper layers, but only slightly influenced stresses (Fig. 3). Thus, average strains and shear moduli reduction values were influenced by resonant effects, whereas average stresses can be considered as parameters, which were less influenced by these effects, and this evidently was the cause of another character of their decrease with distance.

A large scattering in the obtained estimates of parameters of soil response in the near-fault zones testifies to the variety of manifestations of soil response, which depends on the profiling data and on the proximity of a site to an earthquake source. In soft subsurface horizontally layered soils, resonant amplification of seismic waves occurs, and parameters of soil response show certain dependencies on the distance from the fault (or on the level of "input" motion), whereas parameters of the response of "harder" soils are more diverse and cannot be easily approximated by functions of the distance and the level of "input" motion. At the same time, scattering of parameters describing the response of soft soils is strongly related to the level of "input" motion. Closest to the fault plane sites, in water-saturated sandy soils, a noticeable amplification of seismic oscillations occurs at rather large strains (exceeding a certain level of "input" motion) due to pore pressure build-up and transition from "soft-type" nonlinear soil behavior to the "hard-type", as described in PAVLENKO and WEN (2008).

Estimates of nonlinear components of soil response characterize the whole soil thickness down to ~70–80 m. According to the theory of nonlinear interactions, amplitudes of combinational-frequency harmonics generated on the system's nonlinearity are proportional to products of amplitudes of the corresponding interacting normal oscillations (ZAREMBO and KRASIL'NIKOV, 1966). Thus, estimates of quadratic and cubic nonlinear components should be proportional to the second and third powers of the level of "input" motion, respectively. The whole nonlinear component, which includes, among quadratic and cubic, higher-order nonlinearities, should also be proportional to some power of the level of "input" motion (the power is evidently higher than 2 and depends on the contents of nonlinear components of various orders in the system's response). In this case, "input" motion means testing Gaussian white noise signals, which were used for estimating nonlinear components in soil response during the Chi-Chi earthquake. The intensities of the testing signals (influencing the estimates of nonlinear components) were selected so that average stresses and strains induced in soil layers by seismic waves from the earthquake and by testing noise-like signals were as close to each other as possible. The dependencies of the obtained evaluations of nonlinear components in soil response on the levels of testing signals, which were used for the estimations, agree with the theoretical predictions. However, plots in Figure. 5 show other dependencies, such as, the dependencies of the estimated nonlinear components in soil response on the level of preliminary calculated "input" motion from the Chi-Chi earthquake to soil layers, and these dependencies can be roughly approximated by linear functions (a large scattering of

Journal : 24 Dispatch : 17-10-2008 Pages : 24
Article No. : 0401 ☐ LE ☐ TYPESET
MS Code : 0401 ☑ CP ☑ DISK

points around the approximating lines can be partially due to inaccuracies of the estimation methods).

Thus, the estimated values of nonlinear components in soil response show the same regularities as shear moduli reduction values, which also characterize nonlinearity of soil response during a strong earthquake. In papers by PAVLENKO and IRIKURA (2005, 2006), records of the 1995 Kobe and the 2000 Tottori earthquakes were analyzed, and it was shown that shear moduli reduction values expressed in percent approximately coincide with the estimated nonlinear components of soil response. In this work, records of the stronger Chi-Chi earthquake at 31 soil sites are analyzed, and this conclusion is confirmed for the closest to the fault plane sites, where both estimates achieve $\sim$60–80% (Table 1). However, shear moduli reduction values decrease with distance more quickly than estimates of nonlinear components in soil response: At $\sim$35–50 km from the fault ($\sim$1/2 of the length of the fault) shear moduli reduction values and nonlinear components of soil response were $\sim$2–7% and $\sim$10–15%, respectively. Probably, this is partially due to the fact that shear moduli reduction values were estimated for the upper 30 m of soil, whereas estimates of nonlinear components relate to the whole soil thickness ($\sim$70–80 m).

Based on the estimates of shear moduli reduction and the contents of nonlinear components in soil response, we can distinguish the area of strong nonlinearity within $\sim$20–25 km from the fault ($\sim$1/4 of its length). In this area, shear moduli in the upper 30 m of soil reduced by $\sim$40–50% of their initial values during strong motion, and the contents of nonlinear components in soil response were also high, $\sim$40–50% of the whole intensity of the response. This area includes, in particular, the following sites possessing soft subsurface soils: CHY101, TCU110, TCU116, CHY025, TCU065, CHY036, CHY092, CHY104, and TCU115. According to our estimates, at these sites strong ground motion induced changes in rheological properties of the upper layers, and spectra of oscillations on the surface were close to the form $E(f) \sim f^{-n}$.

If we compare soil behavior during the Chi-Chi earthquake (M_w = 7.6), the 1995 Kobe earthquake (M_w = 6.8), and the 2000 Tottori earthquake (M_w = 6.7), we notice that virtually at all studied sites (excluding Port Island) in near-fault zones, hard type of nonlinear soil behavior prevails. Bright examples are SGK site (Kobe earthquake), TTRH02 site (Tottori earthquake); TCU065, TCU102, and TCU110 sites (Chi-Chi earthquake). Strong ground motion led to resonant phenomena in surface soil layers, to large strains and pore-pressure build-up; as a consequence, soil behavior assumed a "hard-type" character, which was particularly expressed nearest the fault planes. In these cases, strong "hard-type" nonlinearity of soil response did not lead to noticeable de-amplification of oscillations on the surface.

Resonant amplification of seismic oscillations in the upper soil layers occurred at many sites during the three earthquakes, however, during the Chi-Chi earthquake, resonant phenomena involved thicker soil layers, down to $\sim$40–60 m (instead of $\sim$10–15 m during the Kobe and Tottori earthquakes), because of the larger magnitude of the Chi-Chi earthquake and the rather homogeneous structure of the upper soil layers down to $\sim$70–80 m at the majority of soil sites.

Journal : 24 Dispatch : 17-10-2008 Pages : 24
Article No. : 0401 ☐ LE ☐ TYPESET
MS Code : 0401 ☑ CP ☑ DISK

On the whole, along with a diversity of manifestations and patterns of soil response depending on many different factors such as the structure of soil layers, their mechanical properties and saturation with water, spectral composition and intensity of the radiation from the earthquake source, we note a similarity in the behavior of similar soils during different strong earthquakes, indicating a fundamental possibility of forecasting soil behavior in future strong earthquakes.

Acknowledgements

This research was a continuation of the research performed together with Prof. K.-L. Wen and supported by the National Science Council (Taiwan) under Grant No. NSC 95-2811-M-492-001. The profiling data at soil stations provided by NCREE are greatly appreciated. The author thanks Prof. K.-L. Wen for his collaboration.

References

Aki, K. and Irikura, K. (1991), *Characterization and mapping of earthquake shaking for seismic zonation*, Proc. 4th Int. Conf. on Seismic Zonation, August 25–29, Stanford, California, 1, 61–110.

Chi, W.-C., Dreger, D., and Kaverina, A. (2001), *Finite-source modeling of the 1999 Taiwan (Chi-Chi) earthquake derived from a dense strong-motion network*, Bull. Seismol. Soc. Am. *91*, 5, 1144–1157.

Idriss, I. M. (1990), *Response of soft soil sites during earthquakes,* Proc. H. Bolton Seed Memorial Symposium (J. M. Duncan, ed.), 2, 273–90.

Lee, W. H. K., Cheng, C.-T., Liao, C.-W., and Tsai, Y.-B. (2001), *Site classification of Taiwan free-field strong-motion stations*, Bull. Seismol. Soc. Am. *91*, 5, 1283–1297.

Lin C.-M., Wen, K.-L., and Chang, T.-M. (2006), *Estimation of S-wave velocity model in the western coastal plain of Taiwan,* Third Intern. Conf. on Urban Earthquake Engineer, Center for Urban Earthquake Engineering, Tokyo, 617–622.

Marmarelis P. Z. and Marmarelis V. Z., *Analysis of Physiological Systems, The White-Noise Approach* (Plenum Press, New York and London 1978), 470 pp.

Pavlenko, O. V. (2001), *Nonlinear seismic effects in soils: Numerical simulation and study*, Bull. Seismol. Soc. Am. *91*, 2, 381–396.

Pavlenko, O. V. and Irikura, K. (2002), *Changes in shear moduli of liquefied and nonliquefied soils during the 1995 Kobe earthquake and its aftershocks at PI, SGK, and TKS vertical array sites*, Bull. Seismol. Soc. Am. *92*, 5, 1952–1969.

Pavlenko, O. V. and Irikura, K. (2003), *Estimation of nonlinear time-dependent soil behavior in strong ground motion based on vertical array data*, Pure Appl. Geophys. *160*, 2365–2379.

Pavlenko, O. V. and Irikura, K. (2005), *Identification of the nonlinear behavior of liquefied and non-liquefied soils during the 1995 Kobe earthquake*, Geophys. J. Intern. *160*, 539–553.

Pavlenko, O. V. and Irikura, K. (2006), *Nonlinear behavior of soils revealed from the records of the 2000 Tottori, Japan, Earthquake at stations of the digital strong-motion network Kik-Net*, Bull. Seismol. Soc. Am. *96*, 6, 2131–2145.

Pavlenko, O. V. and Wen, K.-L. (2008), *Estimation of nonlinear soil behavior during the 1999 Chi-Chi, Taiwan earthquake*, Pure Appl. Geophys. *165*, 373–407.

Roumelioti, Z. and Beresnev, I. A. (2003), *Stochastic finite-fault modeling of ground motions from the 1999 Chi-Chi, Taiwan, earthquake: application to rock and soil sites with implications for nonlinear site response*, Bull. Seismol. Soc. Am. *93*, 4, 1691–1702.

Journal : **24** Dispatch : **17-10-2008** Pages : **24**
Article No. : **0401** ☐ LE ☐ TYPESET
MS Code : **0401** ☑ CP ☑ DISK

STEWART, J. P., LIU, A. H., CHOI, Y., and BATURAY, M. B. (2001), *Amplification Factors for Spectral Acceleration in Active Regions,* Rep. to Pacific Earthquake Engineering Research Center, December 2001, 10.

ZAREMBO, L. K. and KRASIL'NIKOV, V. A. (1966), *Introduction to Nonlinear Acoustics*, Nauka, Moscow.

ZVOLINSKII, N. V. (1982), *Wave processes in non-elastic media*, Problems of Engineering Seismology (in Russian), 23, 4–19.

(Received February 27, 2008, accepted July 7, 2008)